A Letters Journal Exploring
the Frontiers of Physics

OFFPRINT

Superconducting networks with the proximity effect

S. Tsuchiya and S. Tanda

EPL, **94** (2011) 47008

A Letters Journal Exploring the Frontiers of Physics

May 2011

EPL, **94** (2011) 47008
doi: 10.1209/0295-5075/94/47008

www.epljournal.org

Superconducting networks with the proximity effect

S. Tsuchiya[1(a)] and S. Tanda[1,2]

[1] *Department of Applied Physics, Hokkaido University - Sapporo 060-8628, Japan*
[2] *Center of Education and Research for Topological Science and Technology, Hokkaido University Sapporo 060-8628, Japan*

received 30 August 2010; accepted in final form 14 April 2011
published online 18 May 2011

PACS 74.45.+c – Proximity effects; Andreev reflection; SN and SNS junctions
PACS 74.78.-w – Superconducting films and low-dimensional structures

Abstract – We report on the first observation of a novel type of superconducting proximity network using a superconductor-normal metal bilayer. Little-Parks oscillation measurements show that the superconducting current flows through a path enclosed by the edge rather than by the center of the Pb/Au wire in the network. Furthermore, several peaks were observed in a power spectrum analysis. We observed that the sequence of these peaks and that of the monolayer network were connected by the power function, which is a factor of the line width, $S_{B_n} = \alpha^{n-2} S_{A_n}$. This suggests that even in a proximity network vortices are arranged in a way identical to a monolayer network.

Introduction. – A network is a topological concept that represents the connectivity between nodes and branches. This concept has been applied in various fields to, for example, an electrical circuit, a molecular structure, and computer networks. Their properties are beneficially affected by the connectivity of the network. However, networks provide no information about their length, width, and the curves of branches.

Superconducting networks, which consist of multiply connected thin superconducting wires, are typical examples of such networks. In superconducting networks, the network structure has a beneficial effect on the physical properties, because this system is sensitive to the phase coherence of the order parameter over the network. In fact, a phase interference phenomenon, which is known as Little-Parks oscillation, is driven by a magnetic field [1]. Characteristic vortex configurations occur in various network geometries [2–13]. So we can observe the effect on the network as dips or cusps of variations in the magnetic field responses.

Monolayer wire networks have generally been used in previous research. In such systems, the amplitude of the order parameter $|\Psi|$ has the same value along the width direction because the line width d is sufficiently smaller than the coherence length $\xi(T)$ and the penetration depth $\lambda(T)$ ($d \ll \xi, \lambda$). However, for a bilayer network using a superconductor-normal metal wire, it is still not clear whether or not the above condition is appropriate [14]. When a superconductor and a normal metal are joined with a good electrical contact, the superconductivity is weakened and induced in the normal metal. This is known as the proximity effect [15]. In this case, since $|\Psi|$ can be modified along the width direction, novel network effects and size effects are expected to occur.

In this paper, we report on a novel kind of superconducting proximity network realized by using a superconductor-normal metal bilayer. Little-Parks oscillation results show that a superconducting current flows through a path enclosed by the edge rather than by the center of the wire, due to the proximity effect. Additionally, even in a bilayer network, vortices are arranged in a way that is analogous with a superconducting monolayer network. The contribution of the proximity effect is that it provides a vortex configuration with topological stability.

Experimental. – For comparison, we fabricated two types of honeycomb network using standard electron beam lithography methods. One consisted of a lead (Pb) monolayer wire, and the other of a Pb-gold (Au) bilayer wire. A 0.01 μm thick Au layer and a 0.1 μm thick Pb layer were thermally evaporated on a SiO_2 substrate and then the resist was lifted off. Figure 1 shows a scanning electron microscope (SEM) image of the sample. The samples have about 2500 cells with a lattice constant of 2 μm and a line width of 0.2 μm.

(a) Present adress: National Institute for Materials Science - Tsukuba, Ibaraki 305-0003, Japan; E-mail: TSUCHIYA.Satoshi@nims.go.jp

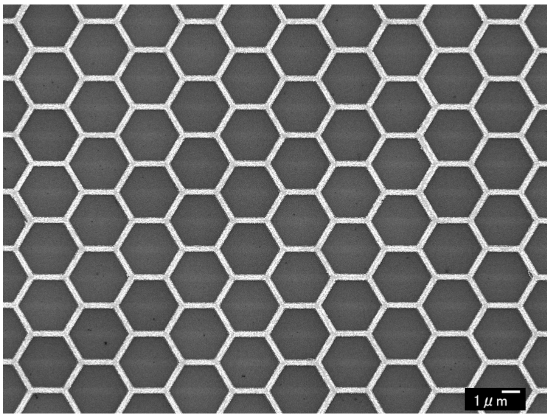

Fig. 1: SEM image of a honeycomb network with about 2500 cells, lattice constant of $2\,\mu$m and line width of $0.2\,\mu$m.

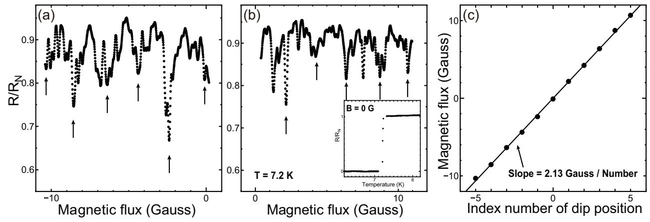

Fig. 2: (a), (b) The magnetic flux dependence of the sample resistance normalized by R_N for the monolayer network. The arrows indicate periodic dips. The inset shows the temperature dependence of the normalized resistance. T_c was observed at around 7.2 K. (c) The index number of the dip positions as a function of magnetic flux. The slope of the line is 2.13 G.

The Little-Parks oscillation is a powerful tool for investigating the configuration of vortices in a network. A Little-Parks oscillation is a periodic variation in T_c with a magnetic field induced by superconducting fluxoid quantization [1]. Specifically, when the temperature is near T_c, the phase coherence of the order parameter is stretched over the entire system. Hence the T_c variation is affected by the vortex configuration. Experimentally a Little-Parks oscillation of the T_c can be observed as a periodic variation in resistance with a magnetic field at a fixed temperature, near the midpoint of the normal-to-superconducting transition. We measured the Little-Parks oscillation of our samples using a 12.5 Hz four-terminal ac resistance bridge with an excitation voltage of $10\,\mu$V. In addition, we performed a spectral analysis using the maximum-entropy method (MEM) to explore certain periods.

Results and discussion. – First, we investigated the monolayer network. The inset in fig. 2(b) shows the temperature dependence of the sample resistance at zero magnetic field, normalized by R_N. The measured T_c is approximately 7.2 K. This value is in good agreement with the T_c of bulk Pb. Figures 2(a) and (b) show the magnetic flux dependence of the normalized resistance in the -10 to 0 and 0 to 10 G ranges at 7.2 K. We found periodic dips

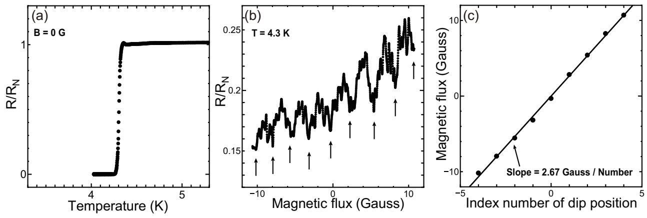

Fig. 3: (a) Temperature dependence of the sample resistance normalized by R_N for the bilayer network. T_c was observed at around 4.3 K. (b) The magnetic flux dependence of the sample resistance normalized by R_N for the bilayer network. The arrows indicate periodic dips. (c) The index number of the dip positions as a function of magnetic flux. The slope of the line is 2.67 G.

as indicated by the arrows. Figure 2(c) shows the index number of the dip positions as a function of the magnetic flux. The slope shows an oscillation period of 2.13 G. The area estimated from the periodicity is $9.72\,\mu\text{m}^2$, and this corresponds to a hexagonal unit cell enclosed by the center of the wire of the network. This value compares well with the value of $9.85\,\mu\text{m}^2$ obtained from a SEM observation with 1.3% accuracy. Thus, the period corresponds to one flux quantum $\Phi_0 = \hbar/2e$ per unit cell.

In contrast, a different period of oscillation was obtained for the bilayer network. Figure 3(a) shows the temperature dependence of the normalized resistance at zero magnetic field resulting in a T_c of approximately 4.3 K. This reduction in T_c suggests that the proximity effect is well induced in the bilayer network [16]. Figure 3(b) shows the magnetic flux dependence of the normalized resistance at 4.3 K. The linear background is the result of the temperature fluctuation with a long period and is related to the used temperature regulation system. Since the fluctuation period is much larger than the measurement time, the fluctuation background changes gradually and linearly in these experiments. Therefore, this background is not intrinsic to the magnetoresistance experiments and does not influence our conclusions. Periodic dips were found as indicated by the arrows. The slope of the line is 2.67 G as shown in fig. 3(c). The area estimated from the period is $7.75\,\mu\text{m}^2$ and corresponds to a hexagonal unit cell enclosed by the edge rather than by the center of the wire in the network. This value compares well with the value of $7.56\,\mu\text{m}^2$ obtained from a SEM observation with 2.4% accuracy. Hence the area of the vortex is different from that of the monolayer network, although both networks have the same honeycomb design. In this case, surface superconductivity can occur, which is nucleated near the sample boundary or around the holes in mesoscopic superconducting systems [17–19]. Generally, surface superconductivity is not expected to occur with a network since the wires of the network are much shorter than the coherence length. In fact, the results for the monolayer network do not indicate surface superconductivity because the current flows in the middle of the wire. However, with the bilayer network, the

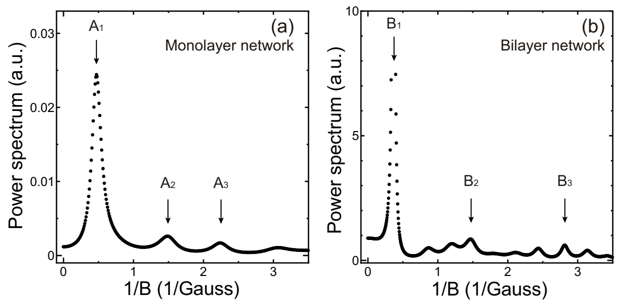

Fig. 4: (a) Power spectrum of the monolayer network. The fundamental peak labeled A_1 corresponds to a period of 2.11 G. The second strongest peak labeled A_2 and the third labeled A_3 correspond to periods of 0.67 and 0.45 G, respectively. (b) Power spectrum of the bilayer network. The fundamental peak labeled B_1 corresponds to a period of 2.71 G. The second strongest peak labeled B_2 and the third labeled B_3 correspond to periods of 0.68 and 0.36 G, respectively.

Table 1: The period and the corresponding area.

	A_1	A_2	A_3	B_1	B_2	B_3
Period (G)	2.11	0.67	0.45	2.71	0.68	0.36
Area (μm^2)	9.81	30.90	46.00	7.64	30.44	57.50

proximity effect modifies the superconducting parameter of the Pb-Au bilayer in terms of the coherence length, penetration depth, and extrapolation length [14]. Therefore, the surface superconductivity provides a possible explanation for these results.

The spectrum analysis was performed using the MEM to explore the network effects. Figure 4(a) shows the power spectrum of the monolayer network, and the complete results are summarized in tables 1 and 2. The fundamental peak labeled A_1 corresponds to a period of 2.11 G, and is consistent with the previous result of 2.13 G. The corresponding area S_{A_1} is 9.81 μm^2. In addition, we observed the second and third strongest peaks, which are 0.67 G and 0.45 G and labeled A_2 and A_3, respectively. The corresponding areas S_{A_2} and S_{A_3} are 30.90 and 46.00 μm^2, respectively. The area ratio is related to the filling ratio of the vortex Φ/Φ_0, which is the magnetic flux Φ in units of the flux quantum Φ_0 per unit cell. S_{A_2}/S_{A_1} and S_{A_3}/S_{A_2} are 3.15 and 1.49, respectively. In particular, since S_{A_2}/S_{A_1} is close to 3, the period of A_2 corresponds in a recent report [20] to the downward cusp in the magnetic field response at $\Phi/\Phi_0 = 1/3$. Thus, these peaks are attributed to the effect of the honeycomb network.

Several peaks were also observed with the bilayer network, as shown in fig. 4(b). The fundamental peak B_1 corresponds to a period of 2.71 G and is consistent with the previous result of 2.67 G. The corresponding area S_{B_1} is 7.64 μm^2. The second and third strongest peaks labeled B_2 and B_3 correspond to periods of 0.68 and 0.36 G, respectively. The corresponding areas S_{B_2} and S_{B_3} are 30.44 and 57.50 μm^2. The ratios S_{B_2}/S_{B_1} and S_{B_3}/S_{B_2} are 3.98 and 1.89, respectively. These ratios are obviously different from those of the monolayer network. Therefore these results indicate the realization of a novel network including the proximity effect.

We should comment on the extra peaks in the bilayer results of the MEM analysis. In the MEM analysis, we need to appropriately determine the correlation range (distance), which is related to spectral resolution, since the peaks that appeared in the MEM spectrum can depend on the value of the correlation range. Therefore, the MEM analysis should be tested for various correlation ranges, and peaks that are independent of the correlation range should be detected as intrinsic peaks. As regards our MEM analysis results, the B_1, B_2, and B_3 peaks are kept for any correlation range and the other peaks are not. So we conclude that the B_1, B_2, and B_3 peaks are intrinsic to the spectrum of the bilayer network.

In what follows we discuss the vortex configuration of these networks at each observed peak. With the monolayer network, vortices are commensurately arranged with their base structures at rational Φ/Φ_0. The geometric ratios S_{A_2}/S_{A_1} and S_{A_3}/S_{A_2} are expected to be 3 and 3/2 because of the honeycomb network. Therefore, the vortex configurations at $\Phi/\Phi_0 = 1$ corresponding to peak A_1, at $\Phi/\Phi_0 = 1/3$ corresponding to peak A_2, and at $\Phi/\Phi_0 = 2/9$ corresponding to peak A_3 are constructed as shown in fig. 5(a), (b), and (c), respectively. The unit cells occupied by vortices are shaded in the figure. The dashed line denotes the path through which the superconducting current flows. At peak A_1, vortices are placed in all the unit cells enclosed by the center of the wire. At peak A_2, one vortex is allocated to every three unit cells. This pattern is commensurately matched with the underlying honeycomb lattice and energetically stable over the whole system. In the same way, a stable vortex configuration is constructed at peak A_3. In comparison with a previous report [20], the 2/9 peak of A_3 appears and the 2/5, 1/2 and 3/5 peaks are absent as filling factors in our experimental data. This disagreement can be attributed to the sample boundary. The boundary of our samples is approximately hexagonal. Since the total size of our samples is smaller than that reported in previous work [13,20], the boundary conditions of the sample can have a considerable effect on the vortex configuration in the network. As regards filling factors 2/5, 1/2 and 3/5, the vortex configuration with the hexagonal symmetry is not constructed. On the other hand, at the 2/9 peak, the vortex configuration is constructed while maintaining the hexagonal symmetry in the same way as the 1 and 1/3 peaks. In our case, the vortex configuration with the hexagonal symmetry can be energetically stable due to the boundary effect. Thus the hexagonal symmetry of the sample edge can induce the 2/9 peak instead of the 2/5, 1/2 and 3/5 peaks. When the sample size becomes large, the 2/5, 1/2 and 3/5 peaks can appear since the boundary condition cannot influence the vortex configuration in the network.

Table 2: The area ratio of the experimental value, geometrically expected value, and our findings.

	S_{A_2}/S_{A_1}	S_{A_3}/S_{A_2}	S_{B_2}/S_{B_1}	S_{B_3}/S_{B_2}	S_{A_1}/S_{B_1}
Experimental value	3.15	1.49	3.98	1.89	1.28
Geometrically expected value	3	$\frac{3}{2}$	3	$\frac{3}{2}$	–
Our findings	–	–	3.11×1.28	1.48×1.28	–

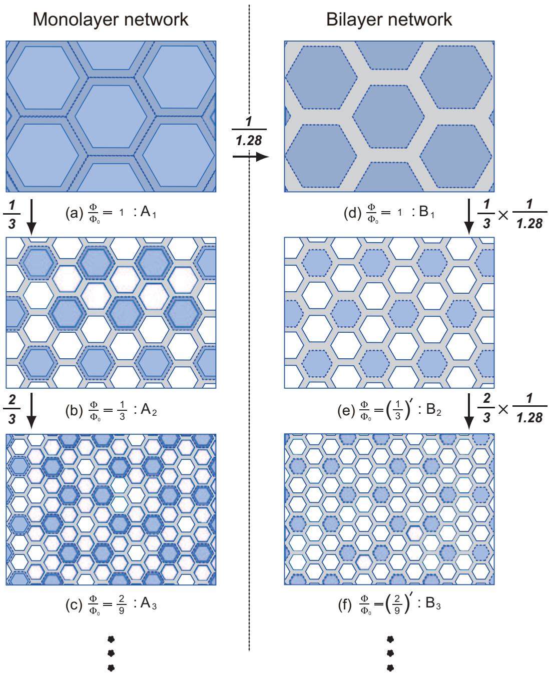

Fig. 5: (Colour on-line) (a)–(c) Vortex configuration of the monolayer network at a magnetic flux corresponding to peaks A_1, A_2, and A_3, respectively. The plaquettes occupied by the vortices are shaded in the figure. The dashed lines denote the loops of the vortices. A vortex consists of a loop enclosed by the center of the wire. (d)–(f) The vortex configuration of the bilayer network at a magnetic flux corresponding to peaks B_1, B_2, and B_3, respectively. A vortex consists of a loop enclosed by the edge of the wire. The arrows and the accompanying values indicate the area ratios.

On the other hand, with the bilayer network, the vortex configuration cannot be constructed from a simple discussion of the vortex area because the area ratio is different from that with the monolayer. In other words, the peaks in the spectrum cannot be explained by the calculation of the geometrical area of the vortex. The geometric area ratios S_{B_2}/S_{B_1} and S_{B_3}/S_{B_2} are expected to be 3 and 3/2, respectively, which are far from the experimental values.

Surprisingly, we found a factor that is associated with the line width in the S_{B_2}/S_{B_1} and S_{B_3}/S_{B_2} ratios (see table 2). The S_{A_1}/S_{B_1} ratio, namely the ratio of the area enclosed by the edge of the wire and the center of the wire, is around 1.28. Then S_{B_2}/S_{B_1} is equal to 3.11×1.28. The value of 3.11 is very close to the S_{A_2}/S_{A_1} value of 3.15. Furthermore S_{B_3}/S_{B_2} is calculated as 1.48×1.28. The value of 1.48 is nearly equal to the S_{A_3}/S_{A_2} value of 1.49. The area ratio of the bilayer network consists of two parts. One is the area ratio of the monolayer network, and the other is the factor of the line width. These relations strongly suggest that the features of the monolayer network could appear even in the bilayer network. That is, the A_1, A_2 and A_3 peaks are expected to correspond to the B_1, B_2 and B_3 peaks, respectively. Therefore, the vortex configurations at the magnetic flux corresponding to peaks B_1, B_2 and B_3 are considered to be as shown in fig. 5(d), (e) and (f), respectively. Even in the bilayer network, vortices are arranged in a way that is analogous with the monolayer network, and the path of the superconducting current is enclosed by the edge of the wire. However, this relation is not derived from a simple discussion of the vortex area. We speculate that the surface superconductivity may be induced by the proximity effect to avoid total energy loss in the entire system.

In addition, a relational expression between S_{B_n} and S_{A_n} is derived from these findings as follows:

$$S_{B_n} = \alpha^{n-2} S_{A_n}. \tag{1}$$

Here S_{A_n} and S_{B_n} represent the sequences $\{S_{A_1}, S_{A_2}, S_{A_3}, \cdots\}$ and $\{S_{B_1}, S_{B_2}, S_{B_3}, \cdots\}$, respectively. α denotes S_{A_1}/S_{B_1}, in other words, the factor of the line width and n is an integer. It is noteworthy that n appears in a power index of α. This fact indicates the contribution of the proximity effect. If only a simple effect of the line width is provided, n cannot appear in the power index. In this case, the factor should be a constant α^{-1} for any n.

The power function of n also suggests the topological stability of the vortex configuration. Because n is considered to be an integer, each state on each n is topologically stable. In fact, according to our vortex configuration model, vortices are correlated with each other and networked on the basis of a triangular lattice that is dual to the honeycomb lattice. The network of arranged vortices is topologically stable because it is maintained regardless of the base network line width. Therefore, a novel kind of superconducting network with the proximity effect is realized in a superconductor-normal metal bilayer network.

Summary. – We demonstrated a new kind of superconducting network with the proximity effect by using Pb-Au bilayer wires. Little-Parks oscillation results showed that the vortex consists of a loop enclosed by the edge of the wire rather than by the center of the wire. This is because the surface superconductivity may be induced by the proximity effect to avoid the total energy loss of the entire system. Furthermore, we observed not only the fundamental peak but also the second and third strongest peaks in the power spectrum analysis. Even in the bilayer network, stable vortex configurations were found to appear at each peak in the same way as in the monolayer network from a comparison with a Pb monolayer network. The contribution of the proximity effect was found to be the power function α^{n-2} in the relation between the S_{B_n} and S_{A_n} sequences. This indicates the topological stability of the vortex configuration. In fact, the network of arranged vortices, which is based on a dual network, is maintained regardless of the line width of the base network. This topological stability of the vortex configuration could be applied to an antidot array system. Furthermore, the effects of the line width could be studied by controlling the proximity effect.

***

We are grateful to K. Inagaki, Y. Asano, and S. Uji for useful discussions. We also thank M. Tsubota, S. Takayanagi, K. Yamaya, and N. Matsunaga for experimental support. This work was supported by a Grant-in-Aid for the 21st Century COE program "Topological Science and Technology" from the Ministry of Education, Culture, Sport, Science and Technology of Japan.

REFERENCES

[1] Little W. A. and Parks R. D., *Phys. Rev. Lett.*, **9** (1962) 279.
[2] de Gennes P. G., *C. R. Acad. Sci. Ser. 2*, **292** (1981) 279.
[3] Simonin J., Rodrigues D. and Lopez A., *Phys. Rev. Lett.*, **49** (1982) 944.
[4] Alexander S., *Phys. Rev.*, **27** (1983) 1541.
[5] Pannetier B., Chaussy J., Rammal R. and Villegier J. C., *Phys. Rev. Lett.*, **53** (1984) 1845.
[6] Gordon J. M., Goldman A. M., Maps J., Costello D., Tiberio R. and Whitehead B., *Phys. Rev. Lett.*, **56** (1986) 2280.
[7] Itzler M. A., Behrooz A. M., Wilks C. W., Bojko R. and Chaikin P. M., *Phys. Rev. B*, **42** (1990) 8319.
[8] Itzler M. A., Bojko R. and Chaikin P. M., *Phys. Rev. B*, **47** (1993) 14165.
[9] Abilio C. C., Butaud P., Fournier Th., Pannetier B., Vidal J., Tedesco S. and Dalzotto B., *Phys. Rev. Lett.*, **83** (1999) 5102.
[10] Lin Y.-L. and Nori F., *Phys. Rev. B*, **65** (2002) 21450.
[11] Sato O., Takamori S. and Kato M., *Phys. Rev. B*, **69** (2004) 092505.
[12] Kasamatsu K., *Phys. Rev. A*, **79** (2009) 021604(R).
[13] Tsuchiya S., Toshima T., Nobukane H., Inagaki K. and Tanda S., *Phys. Rev. B*, **80** (2009) 094502.
[14] Puig T., Rosseel E., Van Look L., Van Bael M. J., Moshchalkov V. V., Bruynseraede Y. and Jonckheere R., *Phys. Rev. B*, **58** (1998) 5744.
[15] de Genns P. G., *Rev. Mod. Phys.*, **36** (1964) 225.
[16] Werthamer N. R., *Phys. Rev.*, **132** (1963) 2440.
[17] Bezryadin A. and Pannetier B., *J. Low Temp. Phys.*, **98** (1995) 251.
[18] Schweigert V. A., Peeters F. M. and Singha Deo P., *Phys. Rev. Lett.*, **81** (1998) 2783.
[19] Bruyndoncx V., Rodrigo J. G., Puig T., Van Look L., Moshchalkov V. V. and Jonckheere R., *Phys. Rev. B*, **60** (1999) 4285.
[20] Xiao Y., Huse D. A., Chaikin P. M., Higgins M. J., Bhattacharya S. and Spencer D., *Phys. Rev. B*, **65** (2002) 214503.